

Bond ionicity and structural stability of some average-valence-five materials studied by x-ray photoemission*†

R. B. Shalvoy,[†] G. B. Fisher,[§] and P. J. Stiles

Department of Physics, Brown University, Providence, Rhode Island 02912

(Received 6 August 1976)

Core-level and valence-band spectra have been obtained by means of x-ray photoemission spectroscopy for the group IV, V, and VI elements Ge, Sn, Pb, As, Sb, Bi, S, Se, and Te and the group IV–VI compounds GeS, GeSe, GeTe, SnS, SnSe, SnTe, PbS, PbSe, and PbTe. These results, taken under ultrahigh-vacuum conditions with unmonochromatized x rays, are presented and discussed in terms of the bonding in materials with an average valence of 5. The effects of relaxation on the chemical shifts are found to be relatively small. The chemical shifts are found to vary in a manner similar to that expected from the magnitude of the elemental electronegativities except for the ordering of the shifts of GeS and GeSe. Relative charge transfers are calculated from the chemical shifts and are found to be in general agreement with ionicities calculated using the Phillips–Van Vechten theory although there is some disagreement as to their magnitudes. A consideration of the structures of the compounds relative to the charge transfers demonstrates the importance of metallic as well as covalent and ionic bonding in determining the most stable structure. The value of critical ionicity carried over from the average-valence-4 materials does not apply to the average-valence-5 materials and this concept does not appear useful in understanding their bonding because of the increased importance of nondirectional metallic bonding.

I. INTRODUCTION

The elements arsenic, antimony, bismuth, and the monochalcogenides of germanium, tin, and lead are members of the family of isomorphous average-valence-5 [abbreviated (5) henceforth] materials. While the average electronic structure is the same within this group,¹ the materials crystallize in three related, but distinct structures² all characterized by sixfold or approximately sixfold coordination. In this paper we discuss the factors responsible for the stability of each of the structural types and the polymorphism between these types^{3–10} in the light of an x-ray photoemission (XPS) study we have conducted. We also compare the results of this study with other physical properties of these materials which are dependent on ionicity.

II. BACKGROUND

Phillips and Van Vechten have successfully applied a model based on spectroscopic properties to derive the coordination of the stable structural forms of average-valence-4 [henceforth (4)] materials based on a scale of ionicity with a critical ionicity separating tetrahedral from cubic coordination.

It would certainly be useful to be able to predict stable structures from and show their direct relation to spectroscopically determined quantities; we will show, however, that the concept of a critical ionicity is not really applicable to the (5) materials. It is, we believe the presence of three

competing forms of bonding, covalent, ionic, and metallic, which leads to the more complicated situation for the (5) materials and leads to three structures in such similar compounds.

The NaCl structure of the lead compounds, SnTe and GeTe (above 400 °C) is typically characterized as a sixfold coordinated ionic structure which can also be viewed as consisting of two interpenetrating fcc sublattices. The most pure covalent bonding within the (5) materials is represented by the rhombohedral structure of the group-V elements and room temperature GeTe. This structure may be obtained from the NaCl structure by displacing the two sublattices relative to one another along the $\langle 111 \rangle$ axis [see Fig. 1(a)] and by stretching the unit cell along the $\langle 111 \rangle$ axis. These distortions are the basis of GeTe's existence as a binary ferroelectric.¹¹ The orthorhombic structure of the germanium and tin sulfides and selenides is less clearly characterized as ionic or covalent. This structure can be simply derived from the NaCl structure by displacing the two sublattices relative to one another by about 0.05\AA in the $\langle 100 \rangle$ direction of the orthorhombic cell [Fig. 1(b) shows the orthorhombic lattice constants] with the direction of the distortion reversing for every other atomic plane. Pawley,¹² has shown that this distortion provides an antiferroelectric nature for the orthorhombic materials. The orthorhombic materials are also characterized by a double-layered structure resulting in easy cleavage planes [Fig. 1(b)]. It is interesting that each set of double layers shift by about 0.4\AA in the $\langle 100 \rangle$ direction regardless of the ionicity of the bonding.

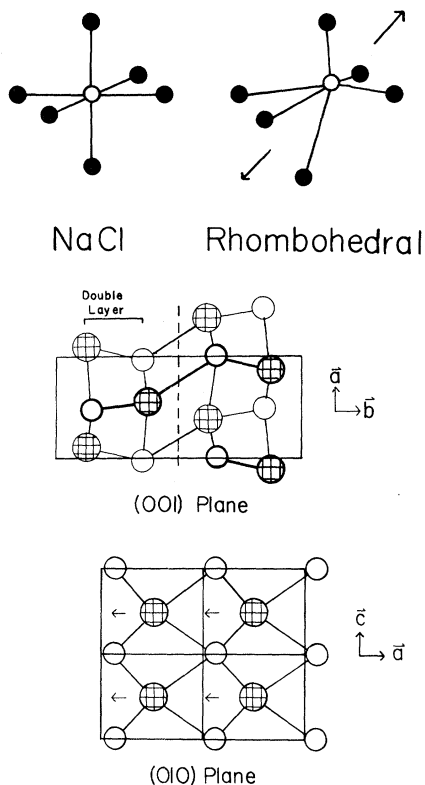


FIG. 1. (a) Representation of the structures. The open circle represents the cation. In this view, the orthorhombic and rhombohedral structures appear similar. (b) The orthorhombic structures of GeS. The dark circles in the upper plane ($\frac{1}{2}\vec{c}$) and the lighter circles are in the lower plane ($0\vec{c}$). Shaded circles represent the cations. The double-layer structure is shown as is the cleavage plane in the (001) plane view. The (010) plane shown is parallel to and just to the left of the cleavage plane. In this view the shifting of the cation sublattice relative to the anion sublattice (as indicated by arrows) can be easily seen as can the four bonds within the layer itself.

The overall similarity of the distorted structures with the NaCl structure can be seen in Fig. 1. Of importance is that the sixfold coordination of the NaCl structure is still maintained to a great extent. The structural parameters are summarized in Table I. In the orthorhombic structure the shortest bond is between the two layers forming the double layers and the longest bond is between the double layers.

A high degree of ionic character is typical for the bonds of an NaCl-type structure. On this basis as well as in response to certain other properties including the high static dielectric constant¹³ and the results of electronic charge-density calculations¹⁴ the bonding in the lead components has been described as predominantly ionic.¹⁵ As we

TABLE I. Materials studied and their room-temperature structures. For the distorted structures there are three long and three short bonds as listed.

Material	Structure	Bond lengths (Å)	Bond angle
As	Rhomb.	2.51, 3.15	84°
Sb	Rhomb.	2.87, 3.37	87°
Bi	Rhomb.	3.10, 3.47	88°
GeS	Ortho.	(2.46, 2.50), (3.20, 3.29)	
GeSe	Ortho.	(2.57, 2.59), (3.32, 3.36)	
GeTe	Rhomb.	2.86, 3.16	88°
SnS	Ortho.	(2.63, 2.68), (3.27, 3.38)	
SnSe	Ortho.	(2.77, 2.82), (3.35, 3.47)	
SnTe	NaCl	3.14	90°
PbS	NaCl	2.97	90°
PbSe	NaCl	3.06	90°
PbTe	NaCl	3.25	90°

have seen however, the covalent group-five elements have a structure that is only a small distortion of the NaCl structure. It is not unreasonable to question therefore whether a large ionic component in the bonding is needed to stabilize the NaCl structure as is the case for the average valence four materials.¹⁶ A number of papers have been published in which ionicities for some or all of these materials have been calculated.¹⁷⁻²⁰ We will consider these results later in comparison with the findings of the XPS study we have performed. We have found a good correlation between some of the ionicity scales and our data as well as the general expectations we have regarding the relative ionicities.

X-ray photoemission spectroscopy was used to determine the core-level binding energies. The photoemitted electron's kinetic energy is determined and from this the initial-state binding energy can be obtained (assuming no relaxation effects for the moment) from Eq. (1):

$$E_{x \text{ ray}} = E_{\text{binding}} + E_{\text{kinetic}} + e\phi_{\text{spect}} + e\psi . \quad (1)$$

The work-function (ϕ_{spect}) and charging (ψ) terms may be accounted for, resulting in a simple relation between the photoelectron kinetic-energy and the initial-state binding energy. The spectrum of emitted electrons versus energy may also contain peaks corresponding to Auger electrons emitted in the deexcitation process of the hole state left by the photoemitted electron. These peaks typically have a more complicated structure than the photoelectron peaks and hence just the energy of the strongest peaks is listed for the Auger transitions.

As first shown by Siegbahn *et al.*,²¹ shifts in the core-level binding energies of an atom correlate well with changes in its chemical environment.

These changes can be described as resulting from charge transfers occurring in the bonding process.^{22,23} Shirley²³ discusses the derivation of a simple model for considering the chemical shifts. By treating the emitting atom as a conducting shell of valence electrons at a radius r surrounding the inner core levels and as part of a lattice with Madelung constant α and nearest-neighbor distance R , the change in internal potential δ as a function of the charge transfer Δq is given by

$$\delta = 14.4\Delta q(1/r - \alpha/R). \quad (2)$$

An important implication of this is that for a given charge transfer, the chemical shift measured will depend on the atomic size. As we are studying atoms from four different rows of the Periodic Table, this effect will be of some concern to us.

III. EXPERIMENTAL

All data were taken on an AEI ES200 electron spectrometer with computer controlled scanning and data acquisition. The vacuum was typically 1×10^{-9} Torr. As the escape depth for electrons of 1000 eV energy is about 10–30 Å, a clean surface and ultra-high vacuum are very desirable. Unmonochromatized magnesium or aluminum radiation was used. Linewidths of these are 0.7 and 1 eV, respectively, which represent the limit on the resolution. The analyzer was a hemispherical electrostatic type with adjustable entrance and exit slits. Sample temperatures of 40 °C during data collection were typical.

Samples were polycrystalline or single crystal (GeS, GeSe, SnS, SnSe) slabs approximately $\frac{1}{2} \times \frac{1}{4} \times \frac{1}{16}$ in. Cleaning was performed in a dry nitrogen-filled Glove Bag by cleaving or scraping followed by immediate insertion through a separately pumped intermediate region into the main vacuum chamber. No further cleaning was required for the sulfides and selenides, and only brief (< 30 sec, 7 μA, 900V) argon ion sputtering was required for the tellurides. The criterion for cleanliness was that the oxygen $1s_{1/2}$ peak be below 1% of the level of the main substrate peak and certainly be less intense than the valence region.

Calibration of the spectrometer was important to enable an accurate set of energy levels to be obtained over an extended period of time. The spacing of the Na $1s$ and $2p$ levels was set to 1041.1 eV,²⁴ and periodically checked. The Au $4f_{7/2}$ level binding energy, relative to the Fermi level of the spectrometer, of 84.0 eV,²⁵ was set prior to each sample run and all energy levels were referenced to it. The Ag $3d_{5/2}$ level was

determined to be 368.2 eV on this scale. To correct for charging effects, a series of small Ag specks were placed on the sample surface following the completion of all other tests and the silver peak's energy measured again as was the energy of the strongest level of the sample. The shift of the silver line from its neutral position was subtracted from the sample levels to correct for charging of the sample. An advantage of this method is that while the silver seen by the spectrometer is chemically separate from the sample, it is in good electrical contact with it. All energies given have been corrected for charging effects.

The comprehensive listing of atomic energy levels given by Bearden and Burr²⁶ was found to be in substantial disagreement (up to 1 eV) with many of our core-level binding-energy measurements made on solid elemental samples. As there was available no complete and accurate listing of the core-level binding energies of interest, these energies were measured prior to the study of the compounds, thereby ensuring that the study of the core-level binding energies and the chemical shifts has been carried out in a complete and consistent manner.

IV. RESULTS

A. Core levels of the elements

The binding energies of most available elemental core levels were measured and are listed in Table II. Energies are known to an uncertainty of ± 0.1 eV. Our findings agree to within that uncertainty with data previously published. For unresolved doublets only the energy of the stronger peak is given. Energies listed are binding energies relative to the Fermi level of gold. Peak width is the full width at half maximum in eV. The unresolved Ge, As, and Se $3d$ levels appear as single asymmetric peaks. The listed energy for these levels is determined from the position of the maximum of the electron energy distribution. As the data for Ge and S were taken using Al radiation, their peak widths are slightly greater than if Mg radiation had been used as was the case for the remaining elemental data.

B. $4p$ levels

The $4p$ levels of the fifth-row elements were observed to be extremely broadened, having widths of 20 eV or more. These broadenings have been further investigated by us²⁷ and a possible mechanism has been proposed.²⁸ A particularly interesting finding that has proved to be useful²⁹ was that for a particular element the width of the peak

TABLE II. Binding energies and the full width at half maximum (FWHM) in eV of the core-electron levels of the elements. Energies are referred to the Fermi level of the spectrometer. The $4p$ levels of Sn, Sb, and Te are discussed in the text.

Level	E	FWHM	Level	E	FWHM	Level	E	FWHM	Level	E	FWHM
Ge			Sn			Pb			S		
$3s \frac{1}{2}$	180.9	3.1	$3p \frac{1}{2}$	756.6	3.5	$4p \frac{1}{2}$	761.5	7.7	$2s \frac{1}{2}$	226.3	2.5
$3p \frac{1}{2}$	125.1	7.7	$3p \frac{3}{2}$	714.7	3.7	$4p \frac{3}{2}$	643.7	5.4	$2p \frac{3}{2}$	162.0	2.2
$3p \frac{3}{2}$	121.2		$3d \frac{3}{2}$	493.4	1.3	$4d \frac{3}{2}$	434.2	4.3			
$3d$	29.0	1.9	$3d \frac{5}{2}$	485.1	1.5	$4d \frac{5}{2}$	412.0	4.2			
<i>(LMM) Auger</i>											
$L_3M_2M_{4,5}$	209.8	4.2	$4s \frac{1}{2}$	137.3	4.4	$4f \frac{5}{2}$	141.7	1.1			
$L_3M_3M_{4,5}$	199.5	5.0	$4p$...		$4f \frac{7}{2}$	136.8	1.0			
$L_3M_{4,5}M_{4,5}$	108.2	1.8	$4d \frac{3}{2}$	25.0		$5p \frac{1}{2}$	106.7	7.6			
$L_2M_{4,5}M_{4,5}$	76.9	1.7	$4d \frac{5}{2}$	24.1	2.15	$5p \frac{3}{2}$	83.3	7.0			
						$5d \frac{3}{2}$	20.6	1.5			
						$5d \frac{5}{2}$	18.0	1.4			
Se			Te			As			Sb		
$3s \frac{1}{2}$	230.1	3.0	$3p \frac{1}{2}$	870.5	3.8	$3s \frac{1}{2}$	204.7	2.6	$3p \frac{1}{2}$	812.9	4.1
$3p \frac{1}{2}$	167.0	2.8	$3p \frac{3}{2}$	819.7	4.1	$3p \frac{1}{2}$	145.7	3.2	$3p \frac{3}{2}$	766.3	3.8
$3p \frac{3}{2}$	161.3	2.5	$3d \frac{3}{2}$	583.5	1.1	$3p \frac{3}{2}$	140.9	2.5	$3d \frac{3}{2}$	537.5	1.2
$3d$	55.2	1.8	$3d \frac{5}{2}$	573.0	1.2	$3d$	41.8	1.6	$3d \frac{5}{2}$	528.2	1.3
			$4s \frac{1}{2}$	169.2	5.8				$4s \frac{1}{2}$	152.8	3.6
			$4p$...					$4p$...	
			$4d \frac{3}{2}$	41.9	1.4				$4d \frac{3}{2}$	33.3	
			$4d \frac{5}{2}$	40.5	1.8				$4d \frac{5}{2}$	32.1	2.4
			Bi						Bi		
$4d \frac{3}{2}$	464.1	5.3	$5p \frac{1}{2}$	119.6	7.0	$4f \frac{5}{2}$	162.2	1.5	$5d \frac{3}{2}$	27.0	1.8
$4d \frac{5}{2}$	440.4	4.9	$5p \frac{3}{2}$	93.0	9.0	$4f \frac{7}{2}$	156.9	1.6	$5d \frac{5}{2}$	24.1	1.6

depended on the chemical state of the element in a manner similar to the chemical shifting of the core level binding energies. Unfortunately, we were not able to utilize this effect here due to interfering peaks in the Sn $4p$ spectrum. These peaks will be discussed in more detail elsewhere.²⁸

C. Core levels and chemical shifts of the (5) compounds

The core-level binding energies and the chemical shifts for the compounds are listed in Table III. Only the stronger levels are listed as the binding energies of the weaker and broader s and p levels in the heavier elements have consequently greater uncertainties which would limit the accuracy of the chemical shifts derived from them.

The Ge $3s_{1/2}$ level in GeSe is obscured by an overlapping Auger electron peak. The basic information on the bond ionicity is contained in the

atomic core-level shifts δ_4 for the cations and δ_6 for the anions. These are given in Table III along with the rms deviation of the individual shifts around the average. An average is taken as no trend in the chemical shifts with binding energy is observed. The uncertainty of any particular chemical shift is 0.1 eV due to uncertainties in the energy calibration and determination.

D. Valence bands

Valence-band spectra were obtained for all materials. Only for Sn and Pb and their compounds was the satellite contribution from high-lying core levels a problem in obscuring the primary valence-band emission. XPS valence-band spectra have been measured with relatively high-resolution monochromatized radiation and reported in the literature for the crystalline group-IV elements,³⁰

TABLE III. Binding energies and FWHM in eV of the electron core levels in the compounds. Shifts of the energies of the levels as compared with those in Table II are shown as δ_4 for the cations and δ_6 for the anions. Auger transition "binding energies" and their respective chemical shifts are given for the germanium compounds. The rms deviation of each chemical shift is also listed.

Level	<i>E</i>	FWHM	δ	Level	<i>E</i>	FWHM	δ				
GeS				GeSe							
Ge3s $\frac{1}{2}$	182.4	3.7	1.5	Ge3s $\frac{1}{2}$							
Ge3p $\frac{1}{2}$	126.8		1.7	Ge3p $\frac{1}{2}$	127.0		1.9				
Ge3p $\frac{3}{2}$	122.7	7.8	1.5	Ge3p $\frac{3}{2}$	123.1	8.0	1.9				
Ge3d	30.5	1.7	1.5	Ge3d	30.9	2.0	1.9				
S2s $\frac{1}{2}$	226.1	2.3	0.2	Se3s $\frac{1}{2}$	229.6	3.8	0.5				
S2p $\frac{3}{2}$	161.8	2.2	0.2	Se3p $\frac{1}{2}$	166.4	3.3	0.6				
δ_4	1.55 ± 0.09	2.2	0.2	Se3p $\frac{3}{2}$	160.9	3.8	0.4				
δ_6	0.2 ± 0.0			Se3d	54.8	2.0	0.4				
				δ_4	1.90 ± 0						
				δ_6	0.48 ± 0.08						
Auger Transition GeS				GeTe							
$L_3M_2M_{4,5}$	212.1		2.3	Ge3s $\frac{1}{2}$	181.9	4.5	1.0				
$L_5M_3M_{4,5}$	201.4		1.9	Ge3p $\frac{1}{2}$	126.0		0.9				
$L_3M_{4,5}M_{4,5}$	109.9		1.7	Ge3p $\frac{3}{2}$	122.1	9.0	0.9				
$L_2M_{4,5}M_{4,5}$	78.6		1.7	Ge3d	30.0	2.0	1.0				
				Te3d $\frac{3}{2}$	583.1	1.4	0.4				
				Te3d $\frac{5}{2}$	572.7	1.5	0.3				
				Te4d $\frac{3}{2}$	41.6		0.3				
				Te4d $\frac{5}{2}$	40.2	2.8	0.3				
				δ_4	0.95 ± 0.05						
				δ_6	0.33 ± 0.04						
Level	<i>E</i>	FWHM	δ	Level	<i>E</i>	FWHM	δ	Level	<i>E</i>	FWHM	δ
SnS				SnSe				SnTe			
Sn3d $\frac{3}{2}$	494.1	1.1	0.7	Sn3d $\frac{3}{2}$	493.9	1.2	0.7	Sn3d $\frac{3}{2}$	493.9	1.6	0.5
Sn3d $\frac{5}{2}$	485.7	1.1	0.6	Sn3d $\frac{5}{2}$	485.7	1.2	0.6	Sn3d $\frac{5}{2}$	485.6	1.6	0.5
Sn4d $\frac{3}{2}$	25.7		0.7	Sn4d $\frac{3}{2}$	25.6		0.6	Sn4d $\frac{3}{2}$	25.4		0.4
Sn4d $\frac{5}{2}$	24.8	2.1	0.7	Sn4d $\frac{5}{2}$	24.7	2.0	0.6	Sn4d $\frac{5}{2}$	24.5	2.3	0.4
S2s $\frac{1}{2}$	225.5	2.2	0.8	Se3s $\frac{1}{2}$	228.6	3.2	1.5	Te3d $\frac{3}{2}$	582.7	1.4	0.8
S2p $\frac{3}{2}$	161.1	2.0	0.9	Se3p $\frac{1}{2}$	165.6	3.2	1.4	Te3d $\frac{5}{2}$	572.3	1.5	0.7
δ_4	0.68 ± 0.04			Se3p $\frac{3}{2}$	159.9	2.9	1.4	Te4d $\frac{3}{2}$	41.3		0.6
δ_6	0.85 ± 0.05			Se3d	53.7	1.8	1.5	Te4d $\frac{5}{2}$	39.9	2.7	0.6
				δ_4	0.63 ± 0.04			δ_4	0.45 ± 0.05		
				δ_6	1.45 ± 0.05			δ_6	0.68 ± 0.08		

TABLE III (Continued)

Level	E	FWHM	δ	Level	E	FWHM	δ	Level	E	FWHM	δ
PbS				PbSe				PbTe			
Pb4d $\frac{5}{2}$	412.6	3.3	0.6	Pb4d $\frac{5}{2}$	412.5	3.1	0.5	Pb4d $\frac{5}{2}$	412.6	4.8	0.6
Pb4f $\frac{5}{2}$	142.4	1.1	0.7	Pb4f $\frac{5}{2}$	142.3	1.1	0.6	Pb4f $\frac{5}{2}$	142.3	1.1	0.6
Pb4f $\frac{7}{2}$	137.6	1.1	0.8	Pb4f $\frac{7}{2}$	137.4	1.1	0.6	Pb4f $\frac{7}{2}$	137.4	1.1	0.6
Pb5d $\frac{3}{2}$	21.3	1.1	0.7	Pb5d $\frac{3}{2}$	21.2	1.1	0.6	Pb5d $\frac{3}{2}$	21.2	1.1	0.6
Pb5d $\frac{5}{2}$	18.8	1.1	0.8	Pb5d $\frac{5}{2}$	18.6	1.1	0.6	Pb5d $\frac{5}{2}$	18.6	1.1	0.6
S2s $\frac{1}{2}$	225.1	1.9	1.2	Se3s $\frac{1}{2}$	228.7	3.3	1.4	Te3d $\frac{3}{2}$	582.4	1.1	1.1
S2p $\frac{3}{2}$	160.8	1.9	1.2	Se3p $\frac{1}{2}$	165.3	3.0	1.7	Te3d $\frac{5}{2}$	572.0	1.2	1.0
				Se3p $\frac{3}{2}$	159.6	3.2	1.7	Te4d $\frac{3}{2}$	41.1		0.8
				Se3d	53.4	2.1	1.8	Te4d $\frac{5}{2}$	39.7	2.6	0.8
δ_4	0.72 ± 0.07			δ_4	0.58 ± 0.04			δ_4	0.6 ± 0		
δ_6	1.2 ± 0			δ_6	1.65 ± 0.15			δ_6	0.93 ± 0.13		

group-V elements,³¹ Te,³² GeTe,³³ SnTe,³⁴ and the lead salts.³⁵ Our results agree substantially with those. Recently we³⁶ and others^{37,38} have reported the valence-band spectrum of various forms of sulfur. Crystalline Se has also been measured.³⁹ Thus, of the materials we've studied in this work, the spectra of the orthorhombic IV-VI compounds, GeS, GeSe, SnS, and SnSe comprise a set of new spectra which will be published elsewhere.⁴⁰

The two lower peaks of the valence band are generally associated with the anion s level (furthest from E_F) and largely cation s level (closer to E_F). Their separation in compounds has been discussed as a measure of ionicity for (4) compounds^{19,41,42} and (5) compounds.¹⁹ In particular, Kowalczyk *et al.*¹⁹ define an ionicity scale based on such separations which we are able to discuss in terms of these new results in Sec. VB 4.

V. DISCUSSION

A. Relaxation energies

It is known that the intra- and interatomic relaxation of electrons around the core-state hole left by the photoemitted electron represents a non-negligible contribution to the energetics of the photoemission process.⁴³ Equation (1) can be restated as

$$E_{x \text{ ray}} = E_{\text{binding}} + E_{\text{kinetic}} + e\phi_{\text{spect}} + e\psi + E_R^*, \quad (3)$$

where E_{binding} is now the actual initial-state binding energy and E_R^* is the relaxation energy. As we are concerned with obtaining the shifts of the initial-state core-level energies, we would like to correct for the changes in the relaxation ener-

gies among the various compounds. Relaxation energies have been calculated for metals⁴³ as well as for free atoms.⁴⁴ The major contributions to the relaxation come from those electrons outside the core level and from the surrounding atoms, particularly in metals.⁴³ We have found that we can estimate the changes of the relaxation energies for atoms in different chemical environments using a model of Wagner and Biloen⁴⁵ and some ideas of Kowalczyk *et al.*⁴³

We will use the cation shift in Ge as the best data is available for this case. The kinetic energy of an LMM Auger electron $E_{LMM}(\text{Ge})$ may be written in a simplified form as⁴⁵

$$E_{LMM}(\text{Ge}) = E(L) - E(M) - E(M) - E_R^*(\text{Ge/Ge}) + E_R^{**}(\text{Ge/Ge}) - \epsilon_A - \phi, \quad (4)$$

where $E(i)$ is the measured binding energy of the i th core level, ϕ the spectrometer work function ϵ_A which represents the coupling of the two-hole states and is assumed to be constant for all compounds with a common photoemitting atom (Ge in this case), and $E_R^*(\text{Ge/Ge})$ represents the relaxation energy of a hole state in a Ge core level where the Ge atom is in a Ge solid. In this notation the chemical shift between the peak's position in Ge and in the compound GeX, where X represents S, Se, or Te can be written as

$$\delta_4^T(\text{GeX, Ge}) = \delta_4^c(\text{GeX, Ge}) - \Delta E_R^*(\text{GeX, Ge}), \quad (5)$$

where δ_4^T is the measured chemical shift, δ_4^c is the chemical shift of the initial-state energies, and

$$\Delta E_R^*(\text{GeX, Ge}) = E_R^*(\text{Ge/GeX}) - E_R^*(\text{Ge/Ge}).$$

Following a suggestion in Kowalczyk *et al.*,⁴³ we use Eq. (4) to state the chemical shift for the Auger electron peaks:

$$\delta E_{LMM} = -\delta_4^T + \Delta E_R^{**}(\text{GeX}, \text{Ge}) - \Delta E_R^*(\text{GeX}, \text{Ge}). \quad (6)$$

Following Wagner and Biloen, we evaluate ΔE_R using Mott and Gurney's expression⁴⁶ for the polarization energy of an ion in a dielectric solid:

$$E_R = \frac{1}{2}(Ne)^2/R(1 - 1/\epsilon_0),$$

where N is the hole charge, R is the effective hole radius (approximately 0.9 the interatomic spacing⁴⁷), and ϵ_0 the optical dielectric constant. The most important parameter is the hole charge N as the other terms vary by 10% or less for these materials. We would like to solve Eq. (6) for E_R^* as we will then be able to evaluate $\delta_4^c(\text{GeX}, \text{Ge})$ in Eq. (5).

As semiconductors will not have complete polarization around the hole state, it is reasonable to assume that $E_R^{**} = 2E_R^*$ indicating a partial polarization ($N^{**} = \sqrt{2}N^*$). We then find

$$\Delta E_R^*(\text{GeX}, \text{Ge}) = \delta E_{LMM}(\text{GeX}, \text{Ge}) + \delta_4^T(\text{GeX}, \text{Ge}) \quad (7)$$

Combining this with Eq. (5) we have an expression for the initial-state energies chemical shift in terms of measured Auger and photoelectron chemical shifts:

$$\delta_4^c(\text{GeX}, \text{Ge}) = 2\delta_4^T(\text{GeX}, \text{Ge}) + \delta E_{LMM}(\text{GeX}, \text{Ge}). \quad (8)$$

Using data in Table III for the germanium compounds we can evaluate these expressions. The systematic variation of the Auger chemical shifts indicates that our expressions of the Auger energies and of the relaxation energies are oversimplified, but in interests of obtaining an estimate, let us take the average of the Auger electron chemical shifts noting that the values in Table III are expressed as binding energies and hence $\Delta E_{LMM} = -\delta_4^T(\text{Auger})$. The results are shown in Table IV.

We see that while the relaxation energies are not negligible, they are small relative to the chemical shifts, and that their inclusion does not change the ordering of the shifts. We do not have satisfactory Auger data for the other atoms, but will assume that the relaxation effects will be small relative to the chemical shifts. The relaxation shift will be small when the element and the compound are in similar electrical environments, GeTe vs Ge, for example. In addition, since the average valence charge densities are more uniform in the tin and lead chalcogenides than in the germanium compounds the changes in relaxation energies will be smaller. Hence, the germanium chalcogenides may represent the most difficult test within these materials and we can conclude

TABLE IV. Parameters found in estimating the shift of the relaxation energies E_R^* .

Compound	$\Delta E_R^*(\text{Ge}/\text{GeX})$	$\delta_4^c(\text{GeX}, \text{Ge})$	$\delta_4^T(\text{GeX}, \text{Ge})$
GeS	-0.35	1.2	1.55
GeSe	-0.2	1.7	1.90
GeTe	0.1	1.0	0.90

that relaxation corrections will not alter the chemical shift ordering or its magnitude appreciably.

B. Charge transfers and ionicity scales

1. Charge transfers

The charge transfer in a partially ionic bond is the basic quantity underlying the chemical shifts, ionicity and other physical parameters. Indeed, Stiles and Brodsky¹⁷ (SB) have shown that within the Phillips-Van Vechten (PVV) approach to chemical bonding in the compounds, the charge transfer is simply related to the ionicity. In principle using Eq. (2) and the relation in SB, chemical shift based ionicities can be determined which can be directly compared to other ionicity parameters. In evaluating Eq. (2), we have assumed that the NaCl structure value for the Madelung constant for all cases as all of the materials are six or near sixfold coordinated and the Madelung constant is only weakly dependent on the coordination. The nearest-neighbor distance R is evaluated for the orthorhombic and rhombohedral structures as an NaCl structure equivalent distance d [$d = (\frac{1}{8} V_{\text{cell}})^{1/3}$]. The initial-charge shell radius r can be evaluated in a number of ways (Slater⁴⁷ or Pauling⁴⁸ atomic radii, or from radial expectation values of free atoms⁴⁹). However, none of these gives a consistent set of values for the charge transfer and unphysical results are encountered often (negative or excessive charge transfers). The problem is that the term $(1/r - \alpha/R)$ is small and very sensitive to small (0.1 Å) changes of r . We will try a slightly different approach which will still allow us to calculate relative but not absolute values of the charge transfers.

We have observed that the relaxation energy correction to the chemical shifts tends to decrease the value for the sulfides and increase the value for the tellurides relative to the values for the selenides. We have observed the opposite effect in applying Eq. (2) to the materials. Hence, we would expect that these two corrections will tend to cancel each other out and give a nearly constant relation between the chemical shift and the charge transfer. Let us then set the term $(1/r - \alpha/R)$ equal to a constant for a given cation or anion. As α/R varies by 7% for a given cation

TABLE V. Ratios of the charge transfers among the compounds possessing a common cation or anion i . The ratio is expressed relative to the compound with the largest chemical shift.

i	(a)			i	(b)		
	S	Se	Te		Ge	Sn	Pb
Ge	0.82...	1.00...	0.50	S	0.17...	0.71...	1.00
Sn	1.00...	0.93...	0.66	Se	0.29...	0.88...	1.00
Pb	1.00...	0.81...	0.83	Te	0.35...	0.73...	1.00

or anion, this assumption is reasonable. Hence, for a given cation or anion i in compound j we can find a set of ratios between chemical shifts of atom i in compounds j and j' , $\delta_{ij}/\delta_{ij'}$, and charge transfers $\Delta q_j/\Delta q_{j'}$, as

$$\delta_{ij}/\delta_{ij'} = \Delta q_j/\Delta q_{j'} \quad (9)$$

We have listed these ratios (in Table V) relative to the largest chemical shift for a given i . We can relate the rows in Table V(a) to each other by use of a row in Table V(b). As the ratios for Ge and Sn are referred to the respective selenide, we will use that row in Table V(b) to scale the rows in Table V(a). As PbS has the largest charge transfer we will relate all other ratios to it for simplicity. Hence, we will multiply the Ge row by 0.23 (0.29×0.81) and the Sn row by 0.71. These results are listed in Table VI.

We have now found a set of relative charge transfers which can be compared to other ionic parameters. The method of reaching these values is not unique, as either the row for $i = S$ or Te in Table V(b) could have used to scale between the rows in Table V(a). However, the use of either of the other rows would not have affected the final results appreciably.

The most basic parameter used in considering bond ionicities in a wide variety of systems is the relative electronegativity difference (ΔX) of the atoms forming the bond.^{48,50} Good correlations have been observed between chemical shifts and ΔX ,²¹ and as the electronegativity differences are small for these materials we expect and have found that the charge-transfer data and the ΔX display similar behavior and trends. These data are plotted in Fig. 2 using the Phillips electronegativities.⁵¹ The Phillips electronegativities

TABLE VI. Charge transfers expressed relative to $\Delta q(\text{PbS})$ which is set as 1.0. The rms deviation of the ratios is also shown.

Ge	0.19 ± 0.01	0.23 ± 0.00	0.12 ± 0.01
Sn	0.77 ± 0.06	0.71 ± 0.06	0.50 ± 0.06
Pb	1.00 ± 0.10	0.81 ± 0.09	0.83 ± 0.06

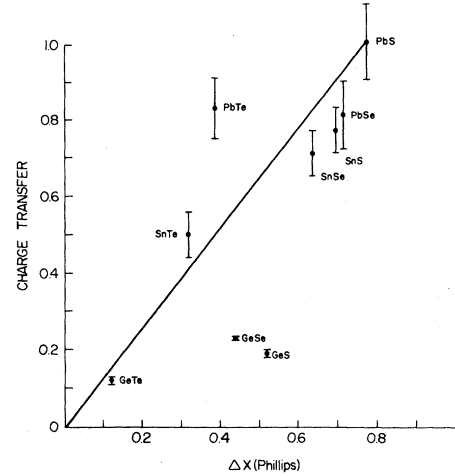


FIG. 2. Charge transfers Δq of the compounds expressed relative to $\Delta q(\text{PbS})$. Compared to the most familiar measure of ionic bonding, the electronegativity difference ΔX , the charge transfers show a fairly good agreement (excepting GeS and GeSe).

are used since the Pauling electronegativities are less discriminating being equal for Ge, Sn, Pb. As the chemical shifts show a clear trend of increasing size from Ge compounds to Pb compounds which is also seen in the Phillips electronegativities, the Phillips scale is used here. Each scale has a telluride compounds with the smallest electronegativity difference, ΔX and places the sulfides and selenides ΔX at similar values.

The charge transfer data show a clear separation between the tellurides and the selenides and sulfides for each cation, while the sulfide and selenide charge transfers are found to be of similar size. A clear separation is also seen between the germanium compound charge transfers and those for the tin and lead compounds. This separation is less pronounced for the telluride Δq however. The main finding from the charge transfer data is that the understanding of bond ionicity based on electronegativity differences is quite good for these materials. If we consider the error bars for each point, excepting GeS and GeSe, all of the charge transfers can be fit by a function linear in ΔX . PbTe is an exception to this statement as well, but a careful consideration of the derivation of $\Delta q(\text{PbTe})$ from the chemical shifts reveals that $\Delta q(\text{PbTe}) < \Delta q(\text{PbSe})$ and hence it will fit the $\Delta q \propto \Delta X$ dependence more reasonably. The deviations of GeS and GeSe from the linear relationship will be considered in connection with the ionicity scales.

Ultimately, the errors of each point limit the fine distinctions that can be made for the charge transfers, but some general conclusions can be

drawn. The ordering of Δq for a common cation R shows $\Delta q(RS) \cong \Delta q(RSe) > \Delta q(RTe)$ and for a common anion X $\Delta q(GeX) < \Delta q(SnX) < \Delta q(PbX)$. However, the charge transfers for PbSe and SnSe are not significantly different.

2. Thermochemical approaches

Thermochemical properties, primarily heats of formation have been the basis for understanding the ionicity of bonds for many years.⁴⁸ Recently, Phillips^{52,53} has shown that the heats of formation for the (4) materials can be derived via a simple relation from the Phillips–Van Vechten ionicity (f_{PVV}). It should be of some interest to see if the heats of formation for the (5) materials correlate with the picture of bond ionicity we have obtained from the charge transfer data.

Experimental data are available for all the compounds. The NBS tables⁵⁴ (supplemented by some recent studies on GeS,⁵⁵ and⁵⁶ SnSe and PbSe) provide the data which is plotted in Fig. 3. A problem encountered is that the heats of formation have relatively large uncertainties as this quantity is the difference of some larger quantities (heat capacities, heats of sublimation, and dissociation energies).

Comparing Figs. 2 and 3 we observe that the heats of formation and the charge transfers follow similar trends although the germanium heats are larger than we would expect considering the charge transfers for these materials. The heat for GeSe appears overly large on this basis. While the inversion between GeS and GeSe is also seen here,

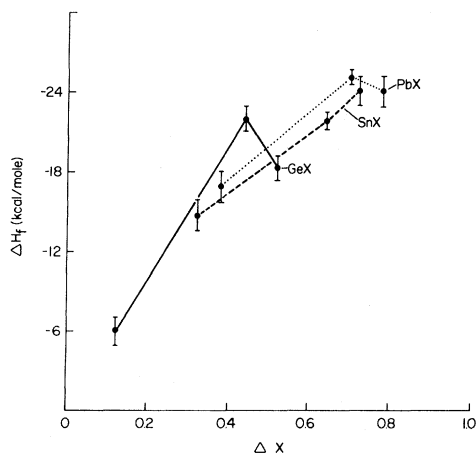


FIG. 3. Heats of formation ΔH_f vs the electronegativity difference. The magnitude of ΔH_f is typically $\frac{1}{3}$ that of similar alkali halides. Data are plotted for a series of compounds with a common cation. PbX, for example, represents the series of compounds PbTe, PbSe, and PbS as the electronegativity of the anion X increases.

the large experimental uncertainties weaken any conclusions that might be drawn from this fact. Over all the heat of formation data are compatible with the charge transfer findings. It is of interest to observe that the heats of formation for the (5) materials are no more than 25 kcal/mole which is much less than that for the corresponding alkali halides such as KBr (79 kcal/mole) or⁵⁷ RbI (94 kcal/mole). This may suggest that while the bonding in the (5) materials has an important ionic contribution, it is not predominantly ionic as the alkali halides are. This finding is reinforced by other XPS measurements. In Refs. 58 and 59 chemical shifts for a wide range of compounds are presented. By comparing that data with the chemical shifts in Table III, it is seen that the chemical shifts for the sulfides are about a factor of two smaller than the corresponding fluorides and a factor of 1.5 smaller than the respective oxides.

Another significant thermochemical quantity which has been associated with ionicity is the cohesive energy of the compound AB, $\Delta G(AB)$.⁵³ $\Delta G(AB)$ is determined as the sum of the cohesive energies of the individual elements plus the free energy of formation of the compound from its elements. The NBS tables⁵⁴ are again used to evaluate this expression. It is found that the free energy of formation is about 0.5 eV less than the corresponding heat of formation and this fact is used to evaluate the expression for GeSe, GeTe, SnS, and SnTe for which values of the free energy of formation is not listed. These values are plotted in Fig. 4.

Phillips⁵³ observed that for (4) materials com-

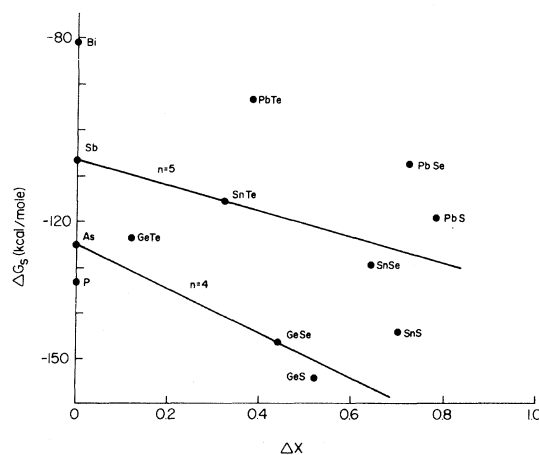


FIG. 4. Cohesive energy ΔG as a function of the electronegativity difference. Where an upward trend with increasing ΔX is seen for the (4) materials, the trend is downward for the (5) materials. n is the principal quantum number of the materials, $n = 5$ includes Sb and SnTe.

posed of atoms in the same row n of the Periodic Table, $\Delta G(AB)$ behaves a function of the row n and the ionicity f_i ,

$$\Delta G(n, f_i) = \Delta G(n, 0)[1 - k(n)f_i]. \quad (10)$$

Skew compounds are observed to have cohesive energies favoring the value predicted for $n = n_B$ (anion). The shift is small (± 6 kcal/mole). We note in particular that increasing ionicity reduces the predicted cohesive energy, a trend which Phillips attributes to shielding of the ionic potential.⁵³ A trend in the $\Delta G(n, 0)$ to smaller values with increasing n may be attributed to the increasing metallization of the bonding for the heavier elements.

If we examine the cohesive energies for the (5) materials as shown in Fig. 4, we first observe that the reduction in the elemental cohesive energies for the heavier elements also occurs. The metallization effect is thus important for the (5) materials. However, we observe that for increasing ionic bonding the cohesive energy increases for materials with atoms all in the same row n . This is just the reverse of the trend observed by Phillips and this difference merits further discussion.

As the ionicity enters into the cohesive energy through the free energy of formation and adds to the cohesive energy in both the (4) and (5) materials^{52,53} it may be that the observed trends result from differences in the covalent part of the bonding. The sp^3 hybrids are particularly strong bonds in comparison with the p bonds of the group-V elements. With this significant difference in bonding, finding a difference in the trends of the cohesive energy is not surprising, although an explanation of the trends is not clear at this point. This result serves as a cautionary reminder that statements valid for the (4) system cannot be generalized to other materials without proof that the extension is justified.

Phillips⁵³ has observed that the quantity $\Delta G(AB) - \Delta G(0)$ increases linearly with ionicity for the (4). As the cohesive energies behave in a quite different manner for the (5), this expectation is not expected to apply to the (5). In fact we have observed that this quantity for the lead compounds is about half that for the corresponding tin and germanium compounds while the charge transfers and the heats of formation for the lead compounds are the largest for a given anion. Hence the extension of this quantity to the (5) materials as a measure of ionicity seems to be unjustified.

3. Spectroscopic approaches based on optical properties

The Phillips-Van Vechten approach to ionicity^{52,60} has been successfully applied to the (4) materials

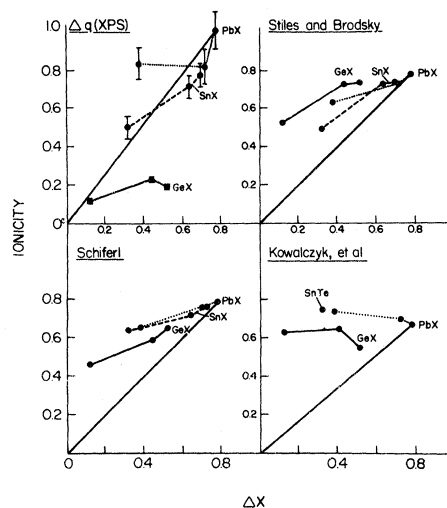


FIG. 5. The ionicities compared. General agreement is seen although there are differences in detail. The prediction of Kowalczyk *et al.* are not as satisfactory as those of the other scales.

and correlated with a wide range of physical properties. This formalism has been extended to the (5) materials by Stiles and Brodsky¹⁷ and Schiferl.²⁰ The results of the calculations for the ionicities are shown Fig. 5 along with the charge transfer data and ionicities calculated from an XPS based approach by Kowalczyk.¹⁹

Stiles and Brodsky¹⁷ (SB) have applied the PVV formalism to the (5) materials by averaging the bond lengths for the non-NaCl structures as

$$a^{-5} = \frac{1}{6} \sum_{i=1}^6 r_i^{-5},$$

and assuming a constant contribution from d -core states (the PVV D parameter). These approximations were tested by varying the factor 5 in the bond length averaging with no appreciable effect, and by applying an effective valence-electron density determined from the experimentally measured plasmon energies in place of that assumed in the constant D and again we found no significant changes.

The SB results are somewhat incomplete given the lack of an ϵ_0 value for GeS and the preliminary values listed for SnS and SnSe. As these points were of particular interest to us after encountering the reversal of charge transfer ordering as mentioned earlier, we investigated the four materials GeS, GeSe, SnS, and SnSe. Their electronic dielectric constants were determined from the ir reflectivity for energies below the band gap.⁶¹ The value of ϵ_0 found for GeS disagrees somewhat with that reported by Gregora,⁶² although the reason for the discrepancy is not clear. Gregora does not show that the difference in ϵ_0 for light

TABLE VII. Corrections to the Stiles and Brodsky ionicities.

Material	ϵ_0	f_i (SB)
GeS	17.8	0.73
GeSe	19.7	0.72
SnS	19.7	0.73
SnSe	21.9	0.72

polarized parallel to the \vec{a} and \vec{c} axes differs by a small but appreciable amount (1 part in 12). As our measurements used unpolarized light it is expected that an average over the two polarizations ϵ_0 is reported here. The completed SB results are listed in Table VII. The complete results are plotted in Fig. 5. The following trends are observed: for a given cation R , $f(RS) = f(RSe) > f(RTe)$ except that $f(PbS) > f(PbSe)$. The ionicities of the sulfides and selenides being nearly constant is quite surprising as there is quite large separation between the germanium compounds and the tin and lead compounds in the charge transfer data. The finding that the ionicity of the tellurides is smaller than that of the sulfides and selenides is in good agreement with the XPS and thermochemical results. However, SB predict a smaller ionicity for SnTe than GeTe, a finding which is in disagreement with both the XPS and thermochemical results.

A comparison of the charge transfer and SB findings reveals that they *are* in agreement with one primary exception: the SB ionicities for the germanium compounds are significantly higher than would be expected given the charge transfers observed. Plots of Δq as the radius parameter is varied in Eq. (2) for common anion series show that for all r , the germanium compound charge transfers are appreciably less than those for the tin and lead compounds. It appears that the SB calculation overestimates the ionicities for these materials.

Van Vechten¹⁶ has observed that the Phillips ionicity parameter C derived from the dielectric constant as in SB also fits a suggestive functional relation for binary compounds AB :

$$C = b(Z_a/r_a - Z_b/r_b)e^{-k_s R} \quad (11)$$

Z_i is the valence of atom i , r_i is the covalent radius as calculated from the bonds lengths,⁶³ R is half the interatomic spacing, k_s is the Thomas-Fermi screening length, and b is adjusted to fit the data derived from the dielectric constant to this equation. In evaluating b , Levine⁶⁴ found that b is constant to within (10–20)% for a given structural type. The expectation is that b is characteristic of a given structural type, and

hence if b is known, Eq. (11) determines the parameter C independent of the dielectric constant. This would be useful if ϵ_0 were unavailable or not well known. Schiferl²⁰ has applied this technique to the (5) materials.

The results are in good agreement with the electronegativities and to a greater extent with the charge transfers excepting the S-Se inversion. Similar to SB, the Ge compound ionicities are somewhat nearer the Sn and Pb than in the charge transfer data. His findings of $f(\text{GeX}) < f(\text{PbX})$ and $f(\text{RS}) > f(\text{RSe}) > f(\text{RTe})$ are very regular although the Pb and Sn values are effectively equivalent. His ionicities for PbTe and SnTe are much closer than the charge transfers. The magnitudes derived for the ionicities are in agreement with those of SB excepting the Ge compounds. It appears that this approach does give good results for the (5) materials.

A problem with this approach is in the assumptions concerning the b parameter. Its physical meaning is not clear and as an adjustable parameter it introduces a (10–20)% uncertainty to the C parameter which enters the ionicity as a square. Levine⁶⁴ encountered a problem in applying this method to some of the (5) materials in trying to fit b to the PVV ionicity for SnTe and GeTe where large free carrier effects complicate the dielectric constant. He found that the b value had to be changed appreciably to fit Eq. (11) to the ionicities derived from the dielectric constant. Hence b is not strictly a function of the structure and some ambiguity can result. That Schiferl obtains reasonable results show that this method is reasonably valid. However, the b parameter needs further study as to its functional dependence. It does appear preferable if possible, to derive the C parameter directly from the dielectric constant in accordance with the PVV theory.

4. Spectroscopic approaches: The anion-cation valence-level gap approach

Quite a different approach has been taken by Kowalczyk.¹⁹ As the gap between the two lowest valence bands, generally bonding-antibonding “s-like” bands has been observed to behave in a manner similar to the gap E_g in the PVV theory, Kowalczyk proposes to decompose this gap into ionic and covalent parts as Phillips has done to E_g and to derive an ionicity from these parts. The gap, measured between the peaks in the photoemission density of states, does indeed increase with ionicity and decrease with increasing lattice constant for the (4) materials.¹⁹ We have observed similar behavior for the gap in the (5) materials as well.⁴⁰ Others have correlated the

changes in the photoemission density of states gap with the changes in the gap at X in the Brillouin zone and proposed the relation $X_3 - X_1 = C$ for the (4) materials.^{41,42} This is a somewhat different interpretation as the *entire* gap is attributed to ionicity.

The results of Kowalczyk's calculations are plotted in Fig. 5 augmented by our data and calculations for the germanium compounds (see Table VIII). A number of puzzling results are visible. In particular, the ordering of ionicities for a given cation is just the reverse of that seen in the previous scales and in the charge transfers. The ionicity of SnTe > that for PbTe and $f(\text{PbTe}) > f(\text{PbSe}) > f(\text{PbS})$. A similar trend is seen in the germanium compounds. A number of explanations are given for this result, but the only relevant one for the (5) is that an unspecified size effect has come into play. A correction for this appears to be successful, but has a rather arbitrary basis.

The size-effect correction may have an explanation if we consider the differing nature of the states composing the two peaks in the XPS valence-band spectrum. The lowest level, typically about 15 eV below the Fermi level has been shown in charge density calculations to be derived essentially from states which are highly localized on the anion.⁶⁵ In the XPS spectrum this peak appears as distinct and corelike, particularly for the more electronegative anions. The higher peak has been shown to be primarily derived from the cation s states, but it is not unreasonable then that the lower peak may behave as a core level and in particular would be chemically shifted. This shift would tend to reduce the splitting of the s states. The chemical shift is larger in materials with lighter, more electronegative anions and hence the gap size is reduced more in these materials than in those with heavy anions (where the effect is small). This does not deny that the gap increases with ionicity, but that the size of the increase may be reduced somewhat by chemical shift influences on the lower corelike level.

While Kowalczyk has made some progress in quantifying the behavior of the gap between the lower valence bands, the failure of the predictions with regard to the ordering of a series of compounds with a common anion reveals that this picture of the lower valence bands is incomplete. Attention must be given to the effects of changes in hybridization particularly when the theory is applied to a wide range of bond types. The most fundamental point also should be clarified theoretically, that the gap can indeed be decomposed into covalent and ionic parts. The finding that the gap can be attributed to the ionic parameter C mentioned above raises questions about the de-

TABLE VIII. Parameters used in determining F_i^{XPS} for the germanium compounds.

Material	d (Å)	ΔE_s^{XPS}	ΔE_s^c	F_i^{XPS}
GeS	2.74	4.5	2.0	0.56
GeSe	2.84	5.3	1.8	0.66
GeTe	3.01	3.8	1.4	0.63

composition of the gap. Further attention should be devoted to this point.

A critical ionicity is proposed by Kowalczyk for the transition between fourfold and sixfold coordination of the compounds studied and it is shown that this scale does give ionicities that can be divided between the two structural coordinations. This point is used as evidence supporting the validity of the approach. However, including ionicities calculated for the germanium compounds, we find that this critical ionicity fails for all three materials. In fact, including the (5) material ionicities on the same figure with the (4) material ionicities is improper, particularly considering that PbS is listed as the borderline material. The reason is that, as we noted regarding the cohesive energies, the bonding of the (4) materials and the (5) materials is quite different in that sixfold coordination characterizes even the more covalently bonded (5) materials. Hence, less ionicity is needed to obtain an NaCl structure in the (5) materials than in the (4) materials. This distinction is also shown by Mooser and Pearson,⁶⁶ indeed as will be shown in Sec. V C, the idea of a critical ionicity for the (5) is not possible as the structural types depend on a combination of ionic, covalent, and metallic influences for their stability.^{66,67} It should be noted in this connection, that if the (5) materials are excluded from the determination of the critical ionicity given by Kowalczyk *et al.*, its value for the (4) materials can be between 0.67 and 0.75.

C. Structural types and bonding

In considering the relations of the ionic, covalent, and metallic contributions to the bonding and structural stability of the (5) materials, it must be remembered that the purely covalent bonding case for the (5) materials is quite different from that of the (4) materials. This difference significantly affects the consideration of the bonding as the structural changes evidenced within the (5) family are much less pronounced than the tetrahedral-octahedral coordination change seen in the (4) materials.

The source of this difference is that the covalent bonding is basically p^3 vs sp^3 in the (4) materials.⁶⁶

Hence the (5) materials regardless of ionicity show a sixfold or near sixfold coordination (see Fig. 1). The distortion of the bond angles from the 90° of pure p^3 bonds is indicative of some admixture of s states in the bonding. Mooser and Pearson⁶⁸ have noted the effect of the increased electron number density, represented by the average principal quantum number \bar{n} of the valence electrons on the bonding of the (4) materials. For compounds AB where element A is in row n of the Periodic Table and element B is in row n' , \bar{n} is the average of n and n' . The effect is particularly noticeable in the group-IV elements.⁶⁸ The changes in metallization effects observed in the (5) elements are much smaller than those in the (4) materials,²⁰ as the structures have higher coordinations in general than the (4) materials. Nonetheless, we observe that metallization does play a significant role in the structural stability.

Given the tendencies of the ionic and metallic bonding to give a nondirected type of structure, it is not surprising that the heaviest and most ionic compounds assume the NaCl structure. The orthorhombic structure is interesting as it can be found for purely covalent black P, moderately ionic SnSe, and highly ionic TlI.^{2,20} One does observe however, that the distortion of the sublattices within a double layer and the asymmetry in the intra- and inter-double layer bond lengths is reduced with increasing ionicity leaving the relative shifting of the double layers as the only distortion in TlI.

The charge transfers calculated from the chemical shifts are plotted in Fig. 6 versus \bar{n} in a manner similar to that of Mooser and Pearson.⁶⁸ We have found that for these materials the metallization parameter α_m derived in Harrison's bond-orbital model⁶⁹ and \bar{n} vary in a similar manner. Harrison⁶⁹ has discussed the influences on the metallization parameter and has been able to describe certain trends reasonably well. An α_m of about 1 appears to be a dividing point for metallic structures. The α_m and \bar{n} parameters are shown in Table IX. In the table we show that to within 4%, $\bar{n} = 9.35\alpha_m$. While no particular significance is attached to the exact relationship, nonetheless on the basis of the nearly linear relation between α_m and \bar{n} we feel that \bar{n} provides a simple and reasonable measure of the reduced directionality of the bonding. In a sense, each axis in Fig. 6 represents an increasing nondirectionality of bonding with increasing \bar{n} and Δq .

It is seen that each structure occupies a well defined region that is indicative of the forces stabilizing a particular structure. The lines drawn between the regions are only approximate and are based on the abilities of alloys of two

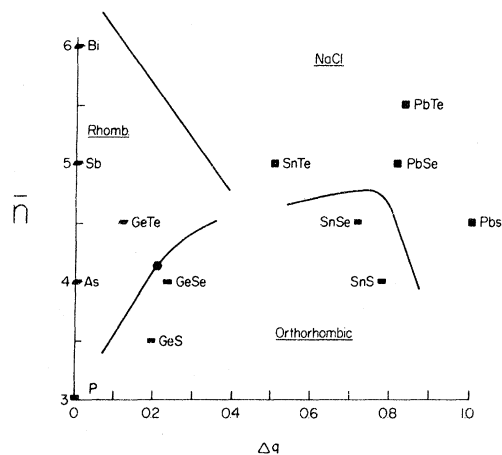


FIG. 6. Charge transfer and covalent bonding for the three structural types. By plotting \bar{n} , the average principal quantum number of the elements and the compounds, against the relative charge transfers Δq , it is seen that each of the three structures is associated with a specific set of \bar{n} and Δq . The lines separating each region are based on the ability of alloys of two neighboring compounds to form single phase systems. The hexagon represents the alloy $\text{GeSe}_{0.8}\text{Te}_{0.2}$ which is discussed in the text.

compounds to form a single phase system.^{70,71}

The well-known finding that the NaCl structured materials correlate with high ionicities and/or large \bar{n} is clearly shown in Fig. 6. Similarly, the rhombohedral structure is assumed by materials with small ionic bonding contributions although we see that even the heaviest materials retain some small s hybridization and that the bonding is not totally delocalized (metallic) as the bond angles still deviate from 90° in Bi. Hence, as is known,⁷² some ionic contribution to the bonding is required to stabilize the NaCl structure in the (5) materials, but the amount required can be small as the distortion from the NaCl structure is not great in the group-V elements. This effect is seen in GeTe which has the

TABLE IX. Bond-orbital-model metallization parameter α_m as a function of \bar{n} .

Material	α_m	\bar{n}	$9.35\alpha_m$
GeS	0.39	3.5	3.65
GeSe	0.42	4.0	3.93
GeTe	0.46	4.5	4.3
SnS	0.44	4.0	4.14
SnSe	0.47	4.5	4.39
SnTe	0.52	5.0	4.86
PbS	0.50	4.5	4.67
PbSe	0.56	5.0	5.24
PbTe	0.57	5.5	5.33

smallest distortion of the rhombohedral structured materials, even though its \bar{n} is smaller than those of Sb and Bi.⁷²

In SnTe however, Δq has become sufficiently large to stabilize the NaCl structure at STP. Further increases in Δq and \bar{n} will only serve to further stabilize the structure although the data on cohesive energies in Fig. 4 indicates that the increasing ionicity is the more significant factor.

In comparison with these familiar results, the forces stabilizing the orthorhombic structure are much less well known. Two observations can be made from Fig. 6. The orthorhombic structure is stable for (i) a wide range of Δq , and (ii) for $\bar{n} < 5$ (the lighter elements). A consideration of the structures of the four compounds stable in this structure reveals that while the distortion within each double layer is reduced for the increased Δq and \bar{n} , the relative shifting of the double layers is only minimally reduced. This relative shifting is a significant feature of the orthorhombic structure. The forces stabilizing this shift are poorly understood. It is significant to observe that Δq for SnS and SnSe is as large as those of PbSe and PbTe and larger than that for SnTe, all of which are NaCl structured. The orthorhombic structure cannot be viewed as a highly covalent structure (unless the bond ionicity of the NaCl structured materials is relatively small), therefore, the sharp cutoff in the orthorhombic region in \bar{n} and the obvious bond distortion even in SnSe indicate that covalent bonding is important in the (5) materials for $\bar{n} < 4.5$. As the shifting of the double layers brings like atomic types into greater proximity, significant ionic character of the bonding in the orthorhombic structure would have a very strong destabilizing influence on the shifts. As this is not observed, we conclude that the bonding for these orthorhombic structured materials is a mixture of ionic and covalent bonding with neither playing a *predominant* role. The shift of double layers is stabilized by the weak covalent bonding

(as the bonds are long) between like atomic types as suggested by Schiferl¹²⁰ and by volume bonding effects (as the orthorhombic structure is preferred over the NaCl structure for these materials when under high pressures, showing that it is a denser structure⁹).

A final conclusion that may be drawn is that the bonding of the (5) materials considered here is *not* predominantly ionic. We have seen that the bonding in the orthorhombic structured materials precludes high ionicities and as the largest charge transfer for the NaCl structured materials (in PbS), is not significantly larger than that in SnS for the orthorhombic structured materials then this final conclusion results. We have seen that while the NaCl structure requires *some* ionic bonding to achieve stability, that contribution need *not* be large, as it is in the alkali halides, as the covalent bonding character results in structures that are only small distortions of the NaCl structure, and the loss of directionality of the covalent bonds for larger \bar{n} also favors the NaCl structure.

D. Polymorphism

As the differences between the structural types are not large, it is not surprising to find a variety of temperature and pressure induced phase transitions between the structures. These are summarized in Table X.

The two transition types have been shown to be ferroelectric (rhombohedral \leftrightarrow NaCl)^{11,12} and antiferroelectric (NaCl \leftrightarrow orthorhombic).¹² We know of no orthorhombic-rhombohedral transitions for these materials. The transition temperature for SnTe has been observed to be dependent on the carrier (holes from Sn vacancies) concentration and hence, the sample stoichiometry.^{73,74} The transition temperature drops as the carrier concentration increases such that for carrier concentrations exceeding $2 \times 10^{20}/\text{cm}^3$ the transition does not occur although some softening of the

TABLE X. Polymorphism occurring under nonstandard temperature or pressure.

Material	STP Structure	Polymorph	Conditions	Reference
GeTe	Rhombohedral	NaCl	$T > 400^\circ\text{C}^a$ $P > 35 \text{ kbar}$	3, 4 6
SnTe	NaCl	Rhombohedral	$T > 100^\circ\text{K}^a$	73, 74
SnS	Orthorhombic	NaCl	$T > 150^\circ\text{C}^a$	9, 10
SnSe	Orthorhombic	NaCl	$T > 200^\circ\text{C}^a$	
SnTe	NaCl	Orthorhombic	$P > 18 \text{ kbar}$	7, 9
PbS	NaCl	Orthorhombic	$P > 25 \text{ kbar}$	7, 9
PbSe	NaCl	Orthorhombic	$P > 42 \text{ kbar}$	7, 9
PbTe	NaCl	Orthorhombic	$P > 43 \text{ kbar}$	7, 9

^aSee discussion in text for details.

phonon mode does occur as the temperature is reduced.^{11,74} This behavior is paralleled in GeTe where the transition temperature varies with sample composition from 390 °C (Te rich) to 460 °C (Ge rich).^{3,4} In view of the very similar behavior of the temperature dependence of the transitions in these two materials, we expect that similar forces are responsible for these transitions, and that they can be treated together.

The pressure induced transition of GeTe to the NaCl structure represents a transition to a more highly coordinated, less distorted structure. This is a familiar effect of high pressures which is also seen in the transition of Sb to a cubic structure under high pressure.⁷⁵

SnTe and GeTe form a single phase system when alloyed that displays smoothly varying lattice constants and bond angles as the alloy composition changes.⁵ The transition temperatures and pressures vary similarly.^{5,76} A $\text{Sn}_{0.625}\text{Ge}_{0.375}\text{Te}$ alloy that has been prepared here has a transition temperature of about 50 °C,⁵ which is convenient for variable-temperature studies. The rhombohedral-NaCl transition temperature is observed to be depressed by increasing numbers of cation vacancies (which also serves to increase the carrier concentration^{5,74}). The lattice constant is reduced by 0.02 Å for samples with the higher carrier concentrations ($10^{21}/\text{cm}^3$). This effect changes the lattice constant much less than the replacement of Ge by Sn atoms in the lattice (0.3 Å) which also serves to depress the transition temperature. We note in summary that the rhombohedral structure is favored for lower sample temperatures and a minimum number of lattice vacancies.

We have already attributed (through Fig. 6) the structural differences between GeTe and SnTe to the greater charge transfer and less directional covalent bonding in SnTe. The chemical shifts of the aforementioned $\text{Sn}_{0.625}\text{Ge}_{0.375}\text{Te}$ alloy have been determined as the sample probe temperature has been varied from -100 to 150 °C (measured by a thermocouple attached to the probe shaft about 0.5 in. from the sample). There is some ambiguity as to the actual temperature of the sample surface due to local heating of the sample surface by the x rays of the spectrometer. For the alloy, we estimate the thermal gradient to be small ~10–20 °C over the probe thermocouple indication. The temperature range scanned at the sample surface should be about -75 to 175 °C. Scanning over the transition temperature, we detected no change in the chemical shifts and hence the charge transfer of the alloy.⁷⁷ This suggests that changes in the ionicity are not the cause of the phase transition. However, a more careful study of this effect would be helpful, particularly in de-

termining the sample surface temperature.

The forces inducing the phase transition have been discussed previously^{5,66} and a suggestion by Krebs⁶⁶ is helpful in understanding the variations in the transition temperature. By considering the potentials of a central Ge atom and two neighboring Te atoms (arranged linearly) he shows that for increasing temperature the Ge atom undergoes increasingly large thermal oscillations these being larger than those of the Te atoms by virtue of its lighter weight. For a certain temperature, the Ge atom will begin to impinge on the repulsive core of the nearer Te atom. The oscillations with increasing temperature will begin to favor the side with the weaker (more distant) repulsive potential and for these temperatures the atom will actually be oscillating about a position symmetric with the neighboring Te atoms. A cubic structure will thus result when the thermal oscillations overcome the directionality of the room temperature bonding. That the structural distortion is small in GeTe allows this transition to occur before the sample decomposes. The transition temperature is much smaller in SnTe as the ionicity and \bar{n} terms are large enough to stabilize the NaCl structure for nearly all temperatures without the aid of thermal oscillations in increasing the nondirectionality of the bonding.

The composition dependent change in the transition temperature may be explained in part from the lattice contraction reducing the temperature required to bring the lattice oscillations into symmetric positions. However, the overall change in the temperature is large compared to the reduction in the lattice constant due to cation vacancies (0.02 Å). It may be that the increased carrier concentration results in a partial delocalization of the valence electrons, thus increasing \bar{n} . This would favor the NaCl structure increasingly for higher carrier concentrations and consequently reduce the temperature required to maintain that structure against the rhombohedral distortion. The transition of the NaCl to the orthorhombic structure initially seems a bit curious as the orthorhombic structure appears to be more directional and less highly coordinated than the NaCl structure. Generally high pressures cause a transition to a more highly coordinated, less directional structure as was observed for the rhombohedral to NaCl structure transition undergone by GeTe for high pressures. Hence we might expect the orthorhombic structure to transform to the NaCl structure under high pressures also recalling that black P transforms under high pressures from the orthorhombic to a cubic structure.⁷⁸

We have already noted that materials in the orthorhombic structure have higher densities than

when in the NaCl structure.⁹ On this basis the transition can be understood. The "nesting"²⁰ of the double layers serves to increase the coordination of the structure which thus becomes favored under high pressures. The black P structure is somewhat different from the IV-VI orthorhombic structure as it is more open and molecular, and hence less highly coordinated.

The reverse of this transition has been observed in that thin films of SnS and SnSe if evaporated onto heated, NaCl substrates grow epitaxially in an NaCl structure (if the substrate is not heated a mixed orthorhombic-NaCl structure results⁹). A lattice expansion is observed to occur, so in effect negative pressure has been applied. The warm substrate and the evaporation onto the NaCl substrate both serve to reduce the directionality of the bonding and hence favor the formation of the NaCl structure if the energy difference between the two structures is not too great. That this is the case is shown by the sensitivity of the resulting structure on the substrate temperature. The difference in the required substrate temperature correlates well with the ionicity difference between SnS and SnSe, the less ionicity, the warmer the substrate must be to obtain nondirectional growth.

It has been reported^{79,80} that the alloy $\text{Ge}_5\text{Se}_4\text{Te}$ crystallizes in a hexagonal structure with a unit cell of five molecules and dimensions $a = 3.82 \text{ \AA}$ and $c = 15.62 \text{ \AA}$. As the two binary compounds (GeSe and GeTe) exhibit cubic symmetry the occurrence of a hexagonal structure is of some interest. In particular can the bonding of this alloy be understood in terms of the mixed ionic-covalent p bonding that has been applied to the three structures of the (5) materials?

The close relationship of the face-centered cubic (fcc) and the hexagonal-close packing (hcp) is well known.² The fcc structure has a stacking order of $ABCABC$ while the hcp has an $ABAB$ stacking order of the atomic planes. Comparison of the structures of the compounds is more complicated, as while the NaCl structure is well defined, the possible hexagonal structures are not so clearly defined. There is a great variety of stacking orders and compositions for the hexagonally structured compounds. The interpretation is further complicated as the exact structure is currently not known due to experimental difficulties.⁸¹

We expect the structure to have sixfold coordination as is found in GeSe and GeTe. The NiAs structure is the most common hexagonal structure with sixfold coordination.^{2,82} However, this structure has only been found for transition metal cations. Additionally, while the cation bonds are of the staggered type as found in NaCl, the anion

bonds are of the eclipsed type. Bonds of this type are not compatible with p bonding. From the description given of the $\text{Ge}_5\text{Se}_4\text{Te}$ alloy^{79,80} it appears that the structure is actually much more complex than the NiAs or other simple structure.

With our present knowledge only a few general remarks may be made. A strictly directional p -bonded model of the structure is not compatible with a hexagonal structure due to the presence in the hexagonal structure of eclipsed bonds. The ionic potential as expressed by Δq in Fig. 6 may be small enough to allow the assumption of an hcp structure (as found for some elements) in a manner similar to GeTe occurring in the rhombohedral structure of the group-V elements, but for this to occur the p character of the covalent bonding would have to be weakened significantly. The occurrence of this structure amongst the cubic structures of the binary compounds remains an interesting problem deserving of further study, particularly as to the importance of the specific composition of the alloy on the bonding.

VI. CONCLUSIONS

We have conducted a comprehensive study of the core-level binding energies and the resulting chemical shifts for the elements Ge, Sn, Pb, As, Sb, Bi, S, Se, and Te and the compounds GeS, GeSe, GeTe, SnS, SnSe, SnTe, PbS, PbSe, and PbTe. After correcting for charging and observing that the relaxation energy corrections are small, we have derived a set of relative charge transfers Δq via a simple potential model.

We have observed that the charge transfers agree with the calculated ionicity scales as to trends between compounds except that the charge transfers for the germanium compounds are significantly smaller than predicted by the ionicity scales. A more careful examination of the derivation of the charge transfers from the chemical shifts supports this finding. Given the magnitudes of the chemical shifts of the IV-VI materials as compared to those for some group-IV halides (PbF_2 for example), we suggested that the bonding did not appear to be *predominantly* ionic.

The extension of the idea of a critical ionicity as used for the (4) materials to the (5) materials as proposed by Kowalczyk is found to be of questionable validity. The (5) materials are nearly sixfold coordinated even for the covalent materials and hence require only a small ionic component in the bonding to stabilize the NaCl structure in contrast to the situation in the (4) materials. Further, as was shown in a consideration of the (5) material polymorphs, the structural stability depends as well on the delocalization of the co-

valent bonding, and on volume bonding effects.

Our discussion of the bonding of the (5) materials is based on the covalent bonding being basically p bonding with some s - p hybridization. In discussing the structures it is concluded that the covalent bonding is important for each polymorph. It was found that loss of directionality, represented by increasing \bar{n} , played a less important role than in the (4) materials, but was an important factor in a description of the structures. Further, it was concluded, particularly in connection with the discussion of the orthorhombic structure that the bonding for the (5) materials in general could not have a predominant ionic character given the obvious covalent bonding present and the destabilizing effect of a large ionic component in the bonding to the relative shifting of the double layers.

The orthorhombic structure was observed to gain further stability from metallic bonding as it has a somewhat greater density than the NaCl structure. This effect increases in significance with the application of high pressures and is seen to be important in stabilizing the NaCl to orthor-

hombic structure transition. It was concluded that as Δq was similar for both the NaCl and orthorhombic structured materials and in the light of the extensive polymorphy observed for the (5) materials, that the three structures are energetically near equilibrium, and hence covalent, ionic, and metallic contributions to the bonding can become significant in stabilizing the structures.

ACKNOWLEDGMENTS

We would like to thank the Materials Research program at Brown University for use of the electron spectrometer. Professor C. Elbaum kindly provided samples of the group-IV elements, and Professor A. Wold and R. Kershaw provided samples of the group-VI elements and grew the GeS and GeSe single crystals and prepared the $\text{Ge}_{0.375}\text{Sn}_{0.625}\text{Te}$ alloy sample. Many helpful conversations with Professor P. Estrup and Dr. S. Nagel are gratefully acknowledged.

- *Submitted by R. B. Shalvoy in partial fulfillment of the requirements for the Ph.D. degree at Brown University.
- †Supported by the Materials Research Laboratory at Brown University funded by the National Science Foundation.
- ‡Present address: Department of Metallurgical Engineering and Materials Science, University of Kentucky, Lexington, Ky. 40506.
- §Present address: Surface Processes and Catalysis Section, National Bureau of Standards, Washington, D. C. 20234.
- ¹Manuel Cardona and D. L. Greenaway, *Phys. Rev.* **133**, A1685 (1964).
- ²R. W. G. Wyckoff, *Crystal Structures*, 2nd ed. (Interscience, New York, 1963), Vol. 1.
- ³K. Schubert and H. Z. Fricke, *Z. Naturforsch. A* **6**, 781 (1951).
- ⁴K. Schubert and H. Z. Fricke, *Z. Metallkd.* **44**, 457 (1953).
- ⁵J. N. Bierly, L. Muldower, and O. Beckman, *Acta Metall.* **11**, 447 (1963).
- ⁶S. S. Kabalkina, L. F. Vereshchagin, and N. R. Serebryanaya, *Zh. Eksp. Teor. Fiz.* **51**, 1358 (1966) [*Sov. Phys.-JETP* **24**, 917 (1967)].
- ⁷J. Kafalas and A. N. Marino, *Science* **143**, 952 (1963).
- ⁸W. Bassett, T. Takahashi, and P. Stook, *Rev. Sci. Instrum.* **38**, 37 (1967).
- ⁹A. N. Mariano and K. I. Chopra, *Appl. Phys. Lett.* **10**, 282 (1967).
- ¹⁰L. Palatnik and V. V. Levitin, *Dokl. Akad. Nauk. SSSR* **96**, 975 (1954).
- ¹¹G. S. Pawley, W. Cochran, R. A. Cowley, and G. Dolling, *Phys. Rev. Lett.* **17**, 753 (1966).
- ¹²G. S. Pawley, *J. Phys. (Paris) Suppl.* **29**, C4-145 (1968).
- ¹³E. Burstein and P. Egli, *Adv. Electron. Electron Phys.* **7**, 1 (1955).
- ¹⁴Y. W. Tsang and M. L. Cohen, *Solid State Commun.* **10**, 87 (1972).
- ¹⁵R. Dalven, *Solid State Phys.* **28**, 179 (1973).
- ¹⁶J. A. Van Vechten, *Phys. Rev.* **182**, 891 (1969).
- ¹⁷P. J. Stiles and M. H. Brodsky, *Solid State Commun.* **11**, 1063 (1972).
- ¹⁸E. Mooser and W. B. Pearson, *J. Electron.* **1**, 629 (1956).
- ¹⁹S. P. Kowalczyk, L. Ley, F. R. McFeely, and D. A. Shirley, *J. Chem. Phys.* **61**, 2850 (1974).
- ²⁰D. Schiferl, *Phys. Rev. B* **10**, 3316 (1974).
- ²¹K. Seigbahn, C. Nordling, A. Fahlman, R. Nordberg, K. Hamrin, J. Hedman, G. Johansson, T. Bergmark, S.-E. Karlsson, I. Lindgren, and B. Lindberg, *ESCA-Atomic, Molecular and Solid State Structure Studied by Means of Electron Spectroscopy* (Almqvist and Wiksells, Uppsala, 1967).
- ²²U. Gelius, *Phys. Scripta* **9**, 133 (1974).
- ²³David A. Shirley, *Adv. Chem. Phys.* **23**, 85 (1973).
- ²⁴N. G. Johnson, *Phys. Rev.* **53**, 435 (1938).
- ²⁵I. Lindau *et al.*, *Phys. Rev. B* **13**, 492 (1976).
- ²⁶J. A. Bearden and A. F. Burr, *Rev. Mod. Phys.* **39**, 125 (1967).
- ²⁷G. B. Fisher, R. Shalvoy, P. J. Estrup, *Bull. Am. Phys. Soc.* **19**, 233 (1974).
- ²⁸G. B. Fisher and R. B. Shalvoy (unpublished).
- ²⁹S. R. Nagel, G. B. Fisher, J. Tauc, and B. G. Bagley, *Phys. Rev. B* **13**, 3284 (1976).
- ³⁰(C, Si, Ge) R. G. Cavell, S. P. Kowalczyk, L. Ley, R. A. Pollak, B. Mills, D. A. Shirley, and W. Perry, *Phys. Rev. B* **7**, 5313 (1973). (Pb) L. Ley, R. A. Pollak, S. P. Kowalczyk, and D. A. Shirley, *Phys.*

- Lett. A 41, 429 (1972).
- ³¹L. Ley, R. A. Pollak, S. P. Kowalczyk, R. McFeely, and D. A. Shirley, Phys. Rev. B 8, 641 (1973).
- ³²M. Schluter, J. D. Joannopoulos, M. L. Cohen, L. Ley, S. P. Kowalczyk, R. A. Pollak, and D. A. Shirley, Solid State Commun. 15, 1007 (1974).
- ³³G. B. Fisher, I. Lindau, B. A. Orłowski, W. E. Spicer, Y. Verhelle, and H. E. Weaver, in *Proceedings of the Fifth International Conference on Amorphous and Liquid Semiconductors*, edited by J. Stuke and W. Brenib (Taylor and Francis, London, 1974), p. 621; G. B. Fisher, I. B. Ortenburger and W. E. Spicer (unpublished).
- ³⁴P. C. Kemeny and M. Cardona, J. Phys. C 9, 1301 (1976).
- ³⁵F. R. McFeely, S. P. Kowalczyk, L. Ley, R. A. Pollak, and D. A. Shirley, Phys. Rev. B 7, 5228 (1973).
- ³⁶G. B. Fisher and R. B. Shalvoy, AIP Conf. Proc. 31, 48 (1976).
- ³⁷W. R. Salaneck, N. O. Lipari, A. Paton, R. Zallen, and K. S. Liang, Phys. Rev. B 12, 1493 (1975); and unpublished.
- ³⁸N. V. Richardson and P. Weinberger, J. Electron Spectrosc. Relat. Phenom. 6, 109 (1975).
- ³⁹N. J. Shevchik, M. Cardona, and J. Tejada, Phys. Rev. B 8, 2833 (1973).
- ⁴⁰R. B. Shalvoy and G. B. Fisher (unpublished).
- ⁴¹W. D. Grobman, D. E. Eastman, and M. L. Cohen, Phys. Lett. A 43, 49 (1973).
- ⁴²D. J. Chadi, M. L. Cohen, and W. D. Grobman, Phys. Rev. B 8, 660 (1973).
- ⁴³S. P. Kowalczyk, L. Ley, F. R. McFeely, R. A. Pollak, and D. A. Shirley, Phys. Rev. B 9, 381 (1974).
- ⁴⁴L. Hedin and A. Johansson, J. Phys. B 2, 1336 (1969).
- ⁴⁵C. D. Wagner and P. Biloen, Surf. Sci. 35, 82 (1973).
- ⁴⁶N. F. Mott and R. W. Gurney, *Electronic Processes in Ionic Crystals* (Clarendon, Oxford, 1948).
- ⁴⁷J. C. Slater, *Quantum Theory of Molecules and Solids* (McGraw-Hill, New York, 1965), Vol. 2.
- ⁴⁸Linus Pauling, *The Nature of the Chemical Bond*, 3rd ed. (Cornell U. P., Ithaca, 1960).
- ⁴⁹C. C. Liu *et al.*, At. Data 3, 1 (1971).
- ⁵⁰J. St. John and A. N. Bloch, Phys. Rev. Lett. 33, 1095 (1974).
- ⁵¹Electronegativities as computed in Ref. 50 and in J. C. Phillips, Phys. Rev. Lett. 20, 550 (1968).
- ⁵²J. C. Phillips, *Bonds and Bands in Semiconductors* (Academic, New York, 1973).
- ⁵³J. C. Phillips and J. A. Van Vechten, Phys. Rev. B 2, 2147 (1970).
- ⁵⁴D. D. Wagman *et al.*, Natl. Bur. Stands. Technical Note 270-3 (U.S. GPO, Washington, D. C., 1968).
- ⁵⁵G. P. Adams, J. L. Margrave, and P. W. Wilson, J. Chem. Thermodyn. 2, 591 (1970).
- ⁵⁶Saleh N. Hejiev, J. Chem. Thermodyn. 2, 765 (1970).
- ⁵⁷O. Kubaschewski, E. L. Evans, and C. B. Alcock, *Metallurgical Thermodynamics*, 4th ed. (Pergamon, New York, 1967).
- ⁵⁸W. E. Morgan and J. R. Van Wazer, J. Phys. Chem. 77, 964 (1973).
- ⁵⁹F. Betts, A. Bienenstock, and C. W. Bates, J. Non-Cryst. Solids 8-10, 364 (1972).
- ⁶⁰J. C. Phillips, Rev. Mod. Phys. 42, 317 (1970).
- ⁶¹J. M. Ziman, *Principles of the Theory of Solids* (Cambridge U.P., Cambridge, 1972).
- ⁶²I. Gregora, B. Velický, and M. Zavetova, J. Phys. Chem. Solids 37, 785 (1976).
- ⁶³J. A. Van Vechten and J. C. Phillips, Phys. Rev. B 2, 2160 (1970).
- ⁶⁴B. F. Levine, J. Chem. Phys. 59, 1463 (1973).
- ⁶⁵M. Schluter, G. Martinez, and Marvin L. Cohen, Phys. Rev. B 11, 3808 (1975).
- ⁶⁶H. Krebs, *Fundamentals of Inorganic Crystal Chemistry* (McGraw-Hill, New York, 1968).
- ⁶⁷G. Lucovsky and R. M. Martin, Phys. Rev. B 8, 5587 (1973).
- ⁶⁸E. Mooser and W. B. Pearson, Acta Crystallogr. 12, 1015 (1959).
- ⁶⁹Walter A. Harrison, Phys. Rev. B 8, 4487 (1973); W. A. Harrison and S. Ciraci, *ibid.* 10, 1516 (1974).
- ⁷⁰H. Krebs, K. Grun, and D. Kallen, Z. Anorg. Allg. Chem. 312, 307 (1961).
- ⁷¹H. Krebs and D. Langner, Z. Anorg. Allg. Chem. 334, 37 (1964).
- ⁷²M. H. Cohen, L. M. Falicov, and S. Golin, IBM J. Res. Dev. 8, 215 (1964).
- ⁷³L. J. Brillson, E. Burstein, and L. Muldawer, Phys. Rev. B 9, 1547 (1974).
- ⁷⁴M. Iizumi, Y. Hamaguchi, K. F. Komatsubara, and Y. Kato, J. Phys. Soc. Jpn. 38, 443 (1975).
- ⁷⁵L. F. Vereshchagin and S. S. Kabalkina, Zh. Eksp. Teor. Fiz. 47, 414 (1964) [Sov. Phys.-JETP 20, 274 (1965)].
- ⁷⁶S. S. Kabalkina, N. R. Serebryanaya, and L. F. Vereshchagin, Fiz. Tverd. Tela 9 (3208) [Sov. Phys.-Solid State 9, 2527 (1968)].
- ⁷⁷R. B. Shalvoy (unpublished).
- ⁷⁸J. C. Jamieson, Science 139, 1291 (1963).
- ⁷⁹J. A. Muir and R. J. Cashman, J. Phys. Chem. Solids 28, 1009 (1967).
- ⁸⁰James A. Muir and Valentin Beato, J. Less Common Metals 33, 333 (1973).
- ⁸¹The structure has not yet been fully characterized, according to J. A. Muir (private communication).
- ⁸²A. Kjekshus and W. B. Pearson, in *Progress in Solid State Chemistry* (Pergamon, Oxford, 1964), Vol. 1.